RSC Pharmaceutics

ROYAL SOCIETY OF CHEMISTRY

PAPER

View Article Online
View Journal | View Issue

Cite this: *RSC Pharm.*, 2024, **1**, 484

A pharmaco–technical investigation of oxaprozin and gaultheria oil nanoemulgel: a combination therapy

Talha,†[a] Ahsan Ali,†[a] Sradhanjali Mohapatra,[a] Ayesha Siddiqui,[a] Uzma Farooq,[a] Athar Shamim,[a] Pooja Jain,[a] Mohammed Aslam,[b] Ramsha Ansari,[a] Mohd. Aamir Mirza*[a] and Zeenat Iqbal*[a]

Worldwide, osteoarthritis is a significant cause of pain, disability, and socioeconomic losses. The disorder's epidemiology is diverse and complicated. Chondrocyte viability and function are compromised by oxidative stress, mechanical stress, and inflammatory mediators. This reprogrammes the cells to undergo hypertrophic differentiation and early "senescence" and increases their susceptibility to pro-catabolic and pro-inflammatory mediators. Given the above discussed pathophysiology of osteoarthritis, it is anticipated that the combination of oxaprozin and gaultheria oil (utilized in traditional medicine for rheumatoid arthritis) will definitely help alleviate the multifactorial disease. The objective of the research was to develop and assess a nanoemulsion gel/nanoemulgel (NEG) by combining oxaprozin, a non-steroidal anti-inflammatory drug (NSAID), and gaultheria oil using Carbopol 974 as a gelling agent. The aqueous titration method was used to create the nanoemulsion by plotting a pseudo-ternary phase diagram, and S_{mix} was used to draw the phase diagram. The formulation was optimized by employing the design of the experiment and incorporated into Carbopol 974 to formulate the NEG. Various properties of the developed formulation, such as the vesicular size, polydispersity index (PDI), zeta potential, morphology and thermodynamic stability, were tested. Furthermore, pH, homogeneity, spreadability, extrudability, texture, bioadhesion, stability, and skin irritation were assessed for the NEG. Additionally, *in vitro* and *ex vivo* tests were conducted for the assessment of the improved formulation. The result shows that the nanoemulsion has a vesicular size of 196.2 nm with good PDI and a zeta potential of –12.33 mV. Furthermore, the results show that the NEG had a biphasic release pattern with a percent cumulative drug release (%CDR) of 78.123 after 25 h. The optimized formulation was also found to be stable at 4 °C for up to 4 weeks. Furthermore, the NEG shows good drug penetration and sustained drug release pattern, which may facilitate the transport of oxaprozin and gaultheria oil through joint tissues, resulting in longer pain alleviation and decreased inflammation. In conclusion, the new formulation would be a good choice for topical medication delivery to improve the oil and oxaprozin combined therapeutic efficacy in the management of osteoarthritis.

Received 16th April 2024,
Accepted 21st May 2024

DOI: 10.1039/d4pm00112e

rsc.li/RSCPharma

1. Introduction

One of the most prevalent degenerative diseases that affect joints and gets worse over time is osteoarthritis, often resulting in chronic pain. The prevalence of this disease is significantly high among adults throughout the world. Osteoarthritis ranks as the second most prevalent rheumatologic condition and is the most common joint disease in India, affecting 22% to 39% of the population. This condition is more prevalent among women than men, with its occurrence significantly rising with age. Approximately 45% of women over 65 experience symptoms, and radiological evidence is present for 70% of individuals in this age group.[1,2] This condition affects the musculoskeletal system and is characterised by the progressive degeneration of articular cartilage, localised inflammation, and debilitating joint pain.[3,4] Since there are no available medications that can alter the course of the disease, symptomatic treatments such as glucocorticoids, monoclonal antibodies, analgesics, and non-steroidal anti-inflammatory drugs (NSAIDs) are commonly prescribed for this condition.[5,6]

[a]*Nanotechnology Lab, Dept of Pharmaceutics, School of Pharmaceutics Education and Research (SPER), Jamia Hamdard, New Delhi, India.*
E-mail: zeenatiqbal@jamiahamdard.ac.in; Tel: +919811733016
[b]*Pharmacy Dept. Tishk International University, Erbil, Kurdistan Region, Iraq*
†Authors share equal contribution.

NSAIDs are commonly used to treat and manage osteoarthritis. Oral NSAIDs are popular among patients, but are linked with serious gastrointestinal side effects (for instance, bleeding, ulceration, and irritation). Hence, numerous research endeavours are focused on devising an effective method of NSAID delivery through topical application to reduce systemic side effects and improve local concentration.[7]

Compared to the oral route, administration through the skin has several advantages, including continuous and smooth delivery of the medication to the site of action without systemic side effects at a comparatively lower dose. A new NSAID belonging to the propionic acid class called oxaprozin is used to treat painful inflammatory conditions associated with osteoarthritis,[8,9] although it comes with some side effects. Moreover, it is a member of BCS Class II, and its inadequate oral absorption capacity may be primarily due to its poor solubility throughout the gastrointestinal tract. Therefore, a topical delivery system is a better option for this drug to increase its efficiency by decreasing the dose and hence side effects. Moreover, topical administration lengthens the contact time, by avoiding the first-pass metabolism.[10] Additionally, a marketed formulation of oxaprozin through topical route is not available.

An innovative drug delivery technique called nano-emulgel (NEG) aims to enhance the therapeutic profile of medications having poor solubility.[11] NEG is an amalgamated preparation of a gel and nanoemulsion (NE). Low viscosity in NEs can result in low retention time and spreadability. However, this can be overcome by incorporating an appropriate gelling agent by forming the NEG. It improves stability, and makes it possible for drugs to be delivered with controlled and immediate release. In comparison to other nano-carrier systems, it is also associated with advantages like a high drug-loading capacity, improved penetration, diffusion, and minimal skin irritation.[12]

One of the main problems associated with NE is stability. An acceptable preparation technique combined with a suitable choice of oils and surfactants is necessary to produce a stable nanoemulsion. Lipid base emulsions are a class of NEs that not only improve drug retention and bioavailability, but also have the ability to dissolve hydrophobic drugs and shield them from enzymatic degradation and dermal hydrolysis. For centuries, gaultheria oil has been utilized in traditional medicine to address conditions associated with inflammation or infection, such as rheumatoid arthritis.[13,14] The primary focus of the pharmacological activities of both pure compounds and crude extract from this genus was on their analgesic and anti-inflammatory characteristics.[15] Gaultheria oil is an essential oil having methyl salicylate as the primary constituent, which is usually used to relieve pain associated with rheumatic arthritis.

This study was conducted to develop a new NEG containing both oxaprozin and gaultheria oil for the treatment of pain related to osteoarthritis using a topical application method. Using the aqueous titration method, gaultheria oil-loaded oxaprozin NE was formulated. Aqueous titration was used to create a pseudo-ternary phase diagram, and S_{mix} was used to draw the phase diagram. The formulation was optimized by employing the design of the experiment (DOE). Finally, NEG was prepared by using Carbopol 974, and characterised and evaluated for its topical application over the skin. Furthermore, the effectiveness of the formulation was confirmed through stability testing *in vitro*, release analysis, *ex vivo* permeation study, and confocal microscopy studies.

The formulation was expected to have a better efficacy owing to the synergistic action of both active components through local application. It would also enhance the patient compliance by decreasing the side effects, as it has a natural component. Furthermore, nanotechnology was exploited for formulating the nanoemulsion, which would definitely increase the skin permeation by reducing the size. This research may open a novel path for utilizing a traditional herbal oil, along with a synthetic drug for osteoarthritis treatment through topical route.

2. Materials and methods

Oxaprozin was procured from Prince Scientific, Hyderabad, India. Gaultheria, sunflower, apricot, lemongrass, clove, and kalonji oils were procured from the local market. The supplier of Carbopol 974® was SD Fine Chemicals India Pvt. Ltd (Mumbai, India). Rhodamine B was sourced from Sigma-Aldrich in Darmstadt, Germany. Surfactants like polyethylene glycol, PEG 400, Tween 20, Tween 40, and Tween 80 were procured from Sisco Research Laboratories Pvt Ltd (Mumbai, India). Solvents like acetone, methanol, and ethanol were supplied by CDH (Delhi, India). Loba Chemie Pvt. Ltd (Mumbai, India) provided the triethanolamine. Other chemicals and all solvents and reagents were of analytical grade.

2.1. Screening of excipients

A number of excipients, including oil, surfactants, and co-surfactants, were thoroughly screened in order to produce a NE. Oils like Gaultheria oil, sunflower oil, apricot oil, lemongrass oil, clove oil, and kalonji oil were screened for the drug's solubility and miscibility before being used in the formulation.[16] The oil with the highest concentration of dissolved oxaprozin was chosen. According to the ionic characteristics and unique HLB values, the surfactants and co-surfactants Tween 20, Tween 40, Tween 80, and PEG-400 were taken into consideration for screening. The HLB value of a surfactant is an important factor in the formulation of emulsions because it enables the choice of an appropriate surfactant or surfactant combination to create a stable emulsion system. The procedure followed in a glass vial, where 1 ml of each of these excipient (oil or surfactant) was added, along with an excess amount of drug. To aid in solubilisation, the materials were vortexed (Remi CM-101 cyclomixer) and kept at 25 °C for 72 min an incubator shaker. The solution's supernatant was extracted after centrifugation (Remi R8C Laboratory centrifuge) at 3000 ± 50 rpm for 10 min and mixed with methanol, and the resultant solution was vortexed and filtered through a 0.22 μm syringe filter. The amount of solubilized drug in the diluted

samples was measured in a UV spectrophotometer (UV 1601, Shimadzu, Japan) at a λ_{max} of 285 nm.[17,18]

2.2. Formulation development

2.2.1. Preparation of a nanoemulsion (o/w type). The aqueous titration method was employed in the construction of a pseudo-ternary phase diagram to ascertain the concentration of different components for the current boundary of NEs.[19] It is a method used to create nanoemulsion regions. It illustrates how volume changes in various phases affect the system's behaviour. The phase diagram was prepared using S_{mix} of Tween 80:PEG 400 in ratios of 1 : 0, 1 : 1, 2 : 1, 3 : 1, and 4 : 1.

Then, in order to cover the study's maximum ratios, the oil phase and S_{mix} were blended at weight ratios of 1 : 9, 2 : 8(1 : 4), 3 : 7(1 : 2.3), 4 : 6(1 : 1.5), 5 : 5(1 : 1), 6 : 4(1 : 0.7), 8 : 2(1 : 0.25), 9 : 1(1 : 0.1), 1 : 2, 1 : 3, 1 : 3.5, 1 : 5, 1 : 6, 1 : 7, and 1 : 8 (w/w). The aqueous titration technique was used to prepare the NE that was previously mentioned. Under moderate agitation, these weight ratios of S_{mix} and oil were diluted dropwise. The mixtures were evaluated visually after being equilibrated, and they were found to be NEs due to their clarity, transparency, and flow ability. Prior to being solubilized in a S_{mix}, the required amount of oxaprozin was first dissolved in a pre-selected oil. A vortex mixer was then used to combine the final mixture. For the characterization studies, nanoemulsions were kept in tightly sealed glass containers at 25 °C.[20]

2.2.2. Optimization of the prepared NE by design of expert (DOE). The Design of Expert (DoE) software (version 132.0.4, Stat-Ease, Minneapolis, MN, USA) was used to optimize the oxaprozin-NE using dependent and independent variables.

In this formulation, the dependent variables were the stirring speed (rpm), oil concentration (%), and surfactant concentration (%), while the independent responses were the particle size (nm), zeta potential (mV) and polydispersity index (PDI). Furthermore, in accordance with the DoE requirements, the oil and surfactant concentrations were chosen at high, medium, and low levels using the ternary phase diagrams. To predict the effects of independent variables on dependent responses, the central composite design (CCD), a response surface methodology approach, was used as the optimization design.[21] A total of fifteen randomised runs were gathered and compared using CCD in order to determine the optimal formulation.[22–24]

2.2.3. Method of preparation of the optimized NE. Using the aqueous titration approach, optimised NEs were created. The drug oxaprozin was dissolved in Gaultheria oil (oil phase). Then, S_{mix} was added while stirring continuously at an ideal speed. The desired mean droplet size of less than 200 nm was then attained by adding distilled water dropwise and stirring moderately. Subsequently, different NE parameters were used to evaluate the optimized formulation.[25]

2.3. Thermodynamic stability stress-stability studies

The screening method was used to determine which formulation was the best and most stable. The stress-stability studies that were conducted on the NEs have the following explanation.

The chosen formulations underwent three cycles of heating and cooling, ranging from 4 to 45 degrees Celsius, and were maintained at each temperature for 48 h. Following the heating–cooling cycle, the formulations underwent physical instability checks for things like flocculation, cracking, phase separation, and precipitation. After passing the first test, the NEs underwent a 30 minute centrifugation at 3500 rpm to make sure the metastable system was ruled out, and to check for any homogeneous changes that might have occurred during the process. Ultimately, the preparations were kept in storage at −21 °C to +25 °C for three cycles of 48 h each. There were variations in the emulsions' homogeneity for Freeze–Thaw cycle.[26,27]

2.4. Characterization of optimized NE

2.4.1. Particle size and polydispersity index (PDI). To learn how NEs behave, the particle size was measured. It was analysed using a zeta-sizer, a computerised assessment system (Malvern Zeta sizer, Nono-ZS, Malvern) that uses DLS software and is founded on the dynamic light scattering (DLS) technology. In order to prepare the formulation for a size analysis of vesicles, it was diluted using distilled water and retained in a quartz cuvette. The study was carried out three times to increase the result consistency.[28]

2.4.2. Zeta potential. The Malvern Zetasizer was also used to measure the zeta potential (Nono-ZS, Malvern computerised inspection system), which is based on the DLS approach and uses DLS software. The zeta potential of the NEs was calculated using the same method as for the particle size measurement. Three runs of the analysis were done to improve the outcome uniformity.[29]

2.4.3. Morphology and size. NE's morphology was observed using transmission electron microscopy (TEM). One drop of the diluted aqueous NE was applied on a copper grid that had been coated with formvar. The grid was then stained with a 2% aqueous solution of phosphotungstic acid (PTA), allowed to dry, and examined under the microscope.[30]

2.5. Preparation of conventional gel

The conventional gel was developed by dispersing oxaprozin (previously solubilized in ethanol) and the gelling agent in water, and continuously stirring at a moderate speed with a magnetic stirrer. Carbopol 974 was accurately weighed out and added in small amounts, while being continuously stirred at 750 rpm until all of the Carbopol was mixed. The necessary amount of the drug solution was added. After allowing the mixture to sit for an entire night, it was neutralised by adding triethanolamine (0.056%) dropwise until the gel was formed. Following preparation, the obtained mixture was examined for colour, appearance, viscosity, and consistency.

2.6. Preparation of the oxaprozin-loaded NEG

Carbopol 974 (0.5%–2%) was precisely weighed and dispersed in water for 6 h. In order to avoid trapping extra air, NE was

also added to the gel gradually, while being continuously agitated at 750 rpm. The mixture was then neutralized by adding dropwise amounts of triethanolamine (0.056%) until the gel had formed. The NEG compositions' consistency, viscosity, colour, and appearance were evaluated after preparation.

2.7. Evaluation of NEG

Gel characterization was done for different parameters.

2.7.1. PH and homogeneity. A calibrated pH meter (biolink PHS-25CW) was used to measure the pH of the nanoformulation at 25 °C, and the homogeneity was visually inspected for aggregates. The analysis was triplicated for better consistency of results.

2.7.2. Drug content. 10 mL of ethanol and 1 g of NEG were constantly mixed for thirty minutes. The mixture's supernatant was collected and passed through a membrane filter with a pore size of 0.45 μm after a 30 minute centrifugation at 3000 rpm. Using an appropriate sample dilution, a triplicate analysis was conducted using a UV spectrophotometer at λ_{max} of 285 nm.[31]

2.7.3. Spreadability and extrudability study. The equipment suggested by Multimar & Co. in 1956 was utilized to gauge the gels' spreadability. A ground glass slide was fixed on a wooden block. A fixed ground slide and another glass slide with the same dimensions were then sandwiched with 1 g of gel, and a 500 g weight was applied to the top of the two slides for a duration of 5 minutes. After a sufficient time, an increase in diameter was observed.[32]

The purpose of the Extrudability Study is to quantify the force needed to extrude the gel from a tube. For this, the emulgel formulation was dispensed into a regular capped collapsible laminate tube and sealed. The weight of the filled tube was measured and noted. The tube was then secured between two glass slides and clamped down. A 500 g weight was placed on top of the glass slide. Subsequently, the cap was opened to allow extrusion of the emulgel. The quantity of emulgel extruded was collected and weighed, enabling the calculation of the percentage of extruded emulgel.

Using the following formula, the extrudability of the optimized formulation was determined:

$$E = M/A$$

where, E = Extrudability, M = Weight is applied to the tube to extrude the gel, A = Area.

2.7.4. Texture analysis of the NEG. The gel's texture properties were evaluated using a Texture Analyzer (TA. XT-Plus from Stable Micro Systems Ltd, Surrey, UK). Approximately 50 mL of the gel formulation was poured into a standard 100 mL beaker, ensuring the absence of air bubbles and achieving a smooth upper surface. A 40 mm diameter disc was then pressed into the gel and withdrawn. The method parameters, including speed rate and insertion depth, were adjusted according to the gel type. Three replicates were conducted for each formulation at room temperature, maintaining consistent measurement conditions. The force-time plot obtained from the analysis was utilized to determine the gel characteristics, such as firmness, consistency, cohesiveness, and work of cohesion.

2.7.5 Rheological behaviour of the NEG. The rheological characteristics of the gel were examined using a Physica MCR 101 Anton Parr controlled stress rheometer. The investigation of the NEG's mechanical characteristics involved flow studies and oscillation tests. The rheometer recorded its mechanical spectra at frequencies between 0.01 to 10 Hz. Using stress sweep tests, the viscoelastic region at 1 Hz was examined. All samples were analysed at 25 °C and 1 °C using spindle number CP50.[34]

2.7.6 Bioadhesive strength measurement. Bioadhesion occurs when an interaction occurs between polymers (present in the gel) and the epithelial surface. It provides information on whether or not our gel can adhere to the skin surface. The bioadhesive strength was measured using a modified technique, and this apparatus has two arm balances. Both ends are secured to glass plates with strings. For measuring the weight, there are two glass plates on one side and one glass plate on the other. We added more weight to the left pan in order to balance the right and left pans. The balance remained in this position for five minutes. A fresh, hairless rat skin piece was held between two glass slides, along with a precisely weighed one-gram NEG. After removing the extra weight from the left pan to stabilize the two glass slides, pressure was added to remove any air that might still be present. For the entire five minutes, the balance was kept in this condition. The left-hand pan was gradually weighted down at a rate of 200 mg per minute until two glass slides got detached from each other. The weight needed to separate the emulgel from the slides was used to calculate the bioadhesive strength.[35] The following formula is used to calculate the bioadhesive strength:

$$\text{Bioadhesive strength} = \text{weight required (in gm)/area (cm}^2\text{)}$$

2.7.7 *In vitro* drug release study. A dialysis membrane was employed for the *in vitro* drug release study. To activate the membrane, the pores were first opened as explained below:

Glycerol was eliminated by washing with running water for 8 h. It was then treated for one minute with 0.3% w/v aq. sodium sulfide solution to remove any remaining sulfur components. Then, the process included acidification with a 0.2% (v/v) sulfuric acid solution, followed by a hot water rinse at 60 °C for 2 minutes to eliminate the acid. Meanwhile, 500 ml of pH 7.4 phosphate buffer (release media) was prepared in accordance with I. P 2007.

The dialysis bag method was utilized, which is a cellulose membrane (Sigma, USA) that permits the free drug to diffuse. The dialysis bag was submerged in release media for 12 h before use. Following the placement of the formulations inside the dialysis bag, it was immersed in 100 ml of release media containing a solvent mixture of 80% (v/v) phosphate buffered saline (PBS) (pH 7.4) and methanol in a beaker. At a temperature of 37 ± 0.05 °C, the beaker was maintained in an incubator shaker operating at 200 rpm. In order to maintain sink conditions, one ml aliquots of the sample were taken at pre-

determined intervals (0, 10, 15, 20, 30, 40, 60, 90, and up to 300 minutes), and an equivalent volume of media was added. Oxaprozin at 285 nm was evaluated using a UV spectrophotometer. The measurement was done in triplicate. The *in vitro* release graph (cumulative percent release) for NEG was calculated.[36] The nanoemulgel (14 mg of oxaprozin) was compared with the nanoemulsion (14 mg of oxaprozin).

2.7.8 *Ex vivo* skin permeation study. A hairless and defatted rat skin was used for study. All animal procedures were performed in accordance with the Guidelines for Care and Use of Laboratory Animals of Jamia Hamdard University, and approved by the Animal Ethics Committee of Jamia Hamdard under registration number 173/GO/RE/S/2000/CPCSEA with approved protocol no. 1977. The rats were housed in a controlled laboratory environment at a temperature of 25 °C ± 1 °C and relative humidity of 55% ± 5%. The sample was kept in a Franz diffusion cell so that the penetration pattern of the drug and the prepared formulations could be measured. In the donor compartments, nanoemulgel (2 g) and nanoemulsion (2 ml) having 14 mg of oxaprozin in the respective samples. While in the receptor compartment, 10 ml of release media as mentioned in the *in vitro* study (pH 7.4) was kept at 37 ± 0.05 °C and continuously stirred at 200 rpm. The aliquot (0.5 mL) was taken out and replaced with a fresh volume of dissolving medium at predetermined intervals. The materials were filtered, diluted, and then examined at 285 nm using a UV spectrophotometer and compared.[36]

2.7.9 Depth of penetration of the formulation into the skin determined by confocal laser scanning microscopy (CLSM). The width and depth of the formulation's skin penetration were measured using the CLSM. For this reason, Rhodamine B dye, a fluorescent probe, was added to the nanoemulgel in place of oxaprozin. A nanoemulsion that contained the same amount of rhodamine dye was allowed to penetrate the skin. Furthermore, the rhodamine solution was also allowed to penetrate the same skin and the results were compared. A portion of slaughtered rat skin was placed between the donor and receptor compartment of the Franz diffusion cell. To avoid contamination and vehicle evaporation, one gram each of the nanoemulgel and an equivalent quantity of nanoemulsion containing the dye were placed in the donor compartments, and covered with Parafilm. The assembly's temperature was kept at 37 ± 0.5 °C. After 8 h, the skin was removed, and any remaining product was washed off with water. Using an argon laser beam with excitation and emission wavelengths of 540 nm and 625 nm, respectively, a CLSM (Olympus Fluo View FV1000, Hamburg, Germany) was utilized to segment, fix, and observe the skin. Infiltration through the stratum corneum is the most difficult aspect of applying topical medication. Absorption through deeper skin layers is simple once the medication or formulation passes through the stratum corneum. Here, the analysis and comparison were done on the basis of intensity and depth of permeation of the dye from NEG, NE and solution.[31]

2.7.10 Skin irritation. A skin irritation test was also performed for the formulations. In this study, patch tests were conducted on the intact skin of Wistar rats to assess the degree of irritation induced by the optimized NEG and NE formulations. The Animal Ethics Committee at Jamia Hamdard (JHAEC) approved the study protocol, and it was registered under registration number 173/GO/RE/S/2000/CPCSEA, 21 December 2022 with approved protocol no. 1977. Three rats (n = 3) from each of the three groups (namely, the control group, the NE group, and the optimised NEG group) were given a cleaned dorsal hair area. The animals were kept in a laboratory setting with controlled temperature (25 °C ± 1 °C and RH 55% ± 5%). The rats' shaven skin was also uniformly treated three times a day with separate doses, *i.e.*, 2 ml of NE having (1 mg mL^{-1}) of oxaprozin and 250 mg of the optimised NEG (containing an equivalent amount of oxaprozin). At 24, 48, and 72 h, the skin was examined for any discernible changes, and a score was assigned. The degree of erythema was measured on a scale from 0 to 4, with weights of 0, 1, 2, 3, and 4 having an erythema scale of zero, mild, moderate, moderate to severe, and severe.[37]

2.7.11 Stability study. To test the stability of the final formulation, NEG was kept at 40 °C ± 0.5 °C for a duration of 4 weeks. As part of the stability assessment, variations in the drug content, PDI, and particle size were measured. Measurements were taken at the end of the 1st, 2nd, 3rd and 4th week.[31]

3 Results and discussion

3.1 Screening of excipients

The investigation of oxaprozin's solubility in different excipients is shown in Fig. 1. Of the experimental oils, Gaultheria oil (3 ± 0.5 mg mL^{-1}) showed the highest solubility of the drug, indicating that it is a suitable oil phase among all the chosen oils for the proposed formulation. Furthermore, it has been exploited in traditional medicine for rheumatoid arthritis, owing to its anti-inflammatory property. Tween 80:PEG 400 were chosen as the surfactant and co-surfactant, respectively, because they demonstrated the highest levels of drug miscibil-

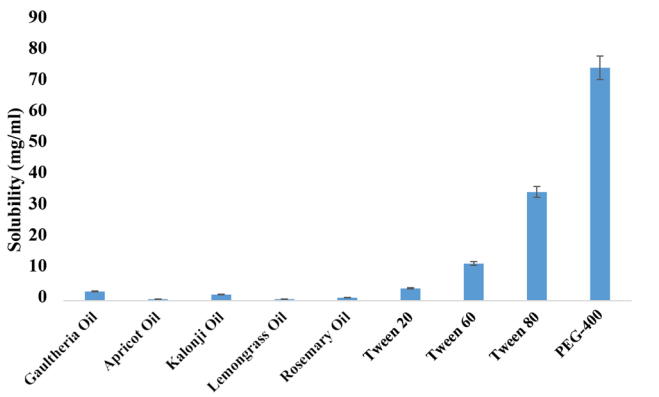

Fig. 1 Solubility tests of oxaprozin in different oils, surfactants and co-surfactants were performed to formulate the NE.

ity and solubility (Fig. 1). In addition, the Tween 80 : PEG 400 combination (S_{mix} ratio) was chosen by using pseudo-ternary phase diagrams to generate a distinct NE with the placebo formulations. Drug solubilization studies are essential to the development of NE because they are vital to the stability, delivery, and upkeep of the formulation. Among other things, choosing the right excipients is essential to creating a homogenous, transparent formulation with a high API binding capacity (Table 1).

3.2 Formulation development

3.2.1 Preparation of a nanoemulsion and excipients optimization. By using an aqueous titration technique and a pseudo-ternary phase diagram, the combination of the selected surfactants was evaluated for the S_{mix} ratio (Fig. 2). These pseudo-ternary phase diagrams were used to select the S_{mix} ratio that should be used to produce a clear, transparent, and homogenous NE. Here, the dotted colour represents a clear NE region. The 2 : 1 S_{mix} pseudoternary phase diagram, which covers the maximum stable o/w NE region, was selected for further study based on the image that comes before it. Whether the NE area is small or large depends on how well that specific surfactant or mixture of surfactants solubilizes the oil phase. A greater solubilization leads to a larger area containing a higher concentration of the transparent, uniform solution.

3.2.2 CCD: mathematical model fitting and optimization of oxaprozin-NE. The particle size (nm), polydispersity index (PDI), and zeta potential (mV) were selected as the independent variables, while the oil concentration (%), surfactant concentration (%), and stirring speed (rpm) were chosen as the dependent responses for the formulation. The oil and surfactant concentrations were determined at high, medium, and low levels using ternary phase diagrams, and the response surface methodology approach known as the CCD optimization design was utilized to predict the effects of independent variables on dependent responses. Following careful consideration of several excipients and their ideal concentrations, a composition appropriate for the preparation of an oxaprozin-NE was chosen. The experimental ranges for the selected independent variables are presented in Table 2. A polynomial quadratic model was found to fit all three dependent responses with a non-significant lack

Table 1 Surfactants with their HLB values for the preparation of S_{mix} ratios

S. no.	Surfactant/co-surfactant	HLB
1	Tween 20	16.7
2	Tween 40	15.6
3	Tween 80	15
4	PEG 400	11.4

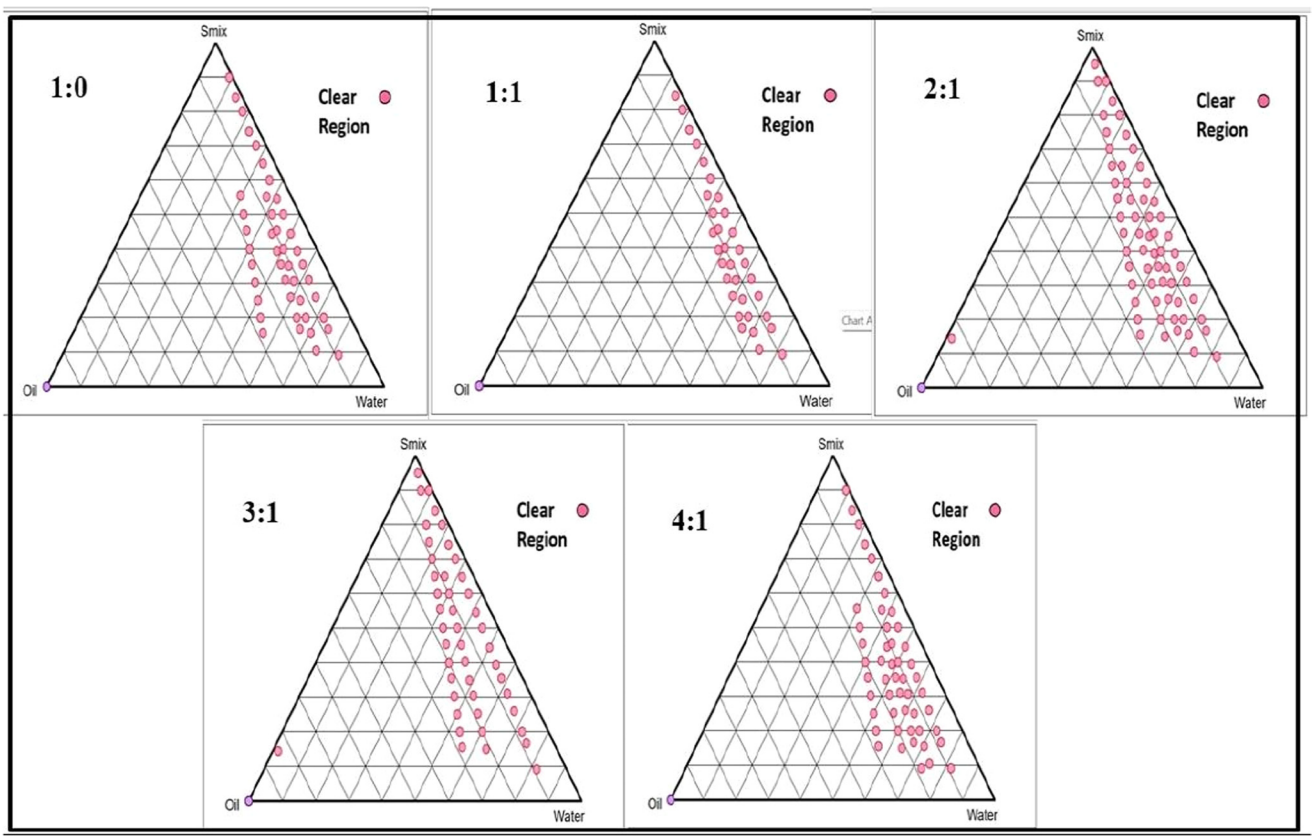

Fig. 2 Software-generated pseudo-ternary phase diagram for identifying the maximum area of the S_{mix} ratio.

Table 2 CCD-based oxaprozin nanoemulsion with independent and dependent variables

Run	Factor 1 A: Oil, %	Factor 2 B: S_{mix}, %	Factor 3 A: Stirring speed (RPM)	Response 1 R1, size	Response 2 R2, zeta potential	Response 3 R3, PDI
1	2.78	14.72	650	223.83	−11.14	0.2888
2	0.56	14.72	300	226.05	−16.51	0.0054
3	0.56	4.44	650	210.2	−9.86	0.2296
4	2.78	4.44	300	260.84	−10.98	0.2482
5	5	4.44	650	250.88	−12.51	0.2043
6	0.56	25	650	190.12	−17.72	0.1758
7	2.78	4.44	1000	196.22	−11.31	0.233
8	2.78	14.72	650	223.83	−11.19	0.2888
9	2.78	14.72	650	223.83	−11.18	0.2888
10	2.78	14.72	650	223.83	−11.14	0.2888
11	2.78	14.72	650	223.83	−11.14	0.2888
12	**2.78**	**25**	**1000**	**183.58**	**−10.21**	**0.2301**
13	5	25	650	195.75	−4.49	0.143
14	2.78	25	300	198.27	−12.1	0.136
15	2.78	14.72	650	223.83	−11.19	0.2888
16	0.56	14.72	1000	189.7	−11.05	0.3294
17	5	14.72	300	246.5	−6.55	0.2609
18	5	14.72	1000	206.58	−10.42	0.0162

of fit ($p > 0.05$), as shown in Table 3. Three-dimensional response surface graphs were created to illustrate how each dependent response interacts with two independent variables in a comparative manner based on the CCD observations (Fig. 3). The comprehensive explanations of each response are provided below.

3.2.3 The impact of independent variables on the vesicular size. The vesicles were between 183.58 and 260.84 nm in size. The surface area increases with decreasing size, ultimately influencing the delivery of the drug, penetration through the skin, and bioavailability. The 3D graphs show the impact of independent factors on the size. The particle size increases with increasing oil concentration because of longer chains, but the vesicle size decreases with increasing surfactant concentration and stirring speed.[38]

3.2.4 The impact of independent variables on the PDI. A PDI represents the consistency of the formulation in terms of the vesicular size. Such a dispersion of the vesicular formulation could impact the drug distribution, and reveal information about their homogeneity and level of aggregation. The CCD graphs demonstrate how each of the three independent variables had a significant impact on the PDI, which was found to be between 0.005 and 0.329. The effect of numerous independent factors on PDI is depicted in 3D graphs in Fig. 3. In the case of an increase in the surfactant concentration, the value of PDI decreases. However, an increase in the oil concentration significantly increases the value of PDI.[39]

3.2.5 The impact of independent variables on the zeta potential. The zeta potential of a formulation indicates its stability. The zeta potential of formulations ranged from −4.49 to −17.72. The zeta potential increases as the amount of oil concentration increases, while the zeta potential falls as the amount of surfactant concentration increases. There is no such variation observed with a change in the stirring speed.[40] The formulation with a vesicular size of 196.22 nm, PDI of 0.233, and Zeta potential of −11.31 was determined to be the optimized formulation after analysing each variable.

3.3 Thermodynamic stability

Studies on the thermal stability, including centrifugation, the freeze–thaw cycle, and heating–cooling, showed that some NE formulations had phase separation and others were turbid (Table 4). The process of Ostwald ripening involves the diffusion of small droplets to form larger droplets or aggregates. This is a free-surface energy process, and may be the cause of this instability. More physical characterization was performed on the formulations that showed no signs of thermodynamic instability.

Table 3 Various levels or experimental ranges for the selected independent variables

	Intercept	A	B	C	AB	AC	BC	A^2	B^2	C^2
R1	183.58	11.5762	−18.8025	−19.8263	−8.7625	0.35	12.4825	−6.35167	−14.0742	−8.36167
p-Values		<0.0001	<0.0001	<0.0001	0.0006	0.8337	<0.0001	0.0034	<0.0001	0.0006
R2	−10.21	2.64625	0.0175	0.39375	3.97	−2.3325	0.555			
p-Values		<0.0001	0.1271	<0.0001	<0.0001	<0.0001	<0.0001			
R3	0.2301	−0.014475	−0.028775	0.01975	−0.001875	−0.142175	0.027325	−0.079737	−0.020885	−0.056075
p-Values		<0.0001	<0.0001	<0.0001	<0.0001	<0.0001	<0.0001	<0.0001	<0.0001	<0.0001

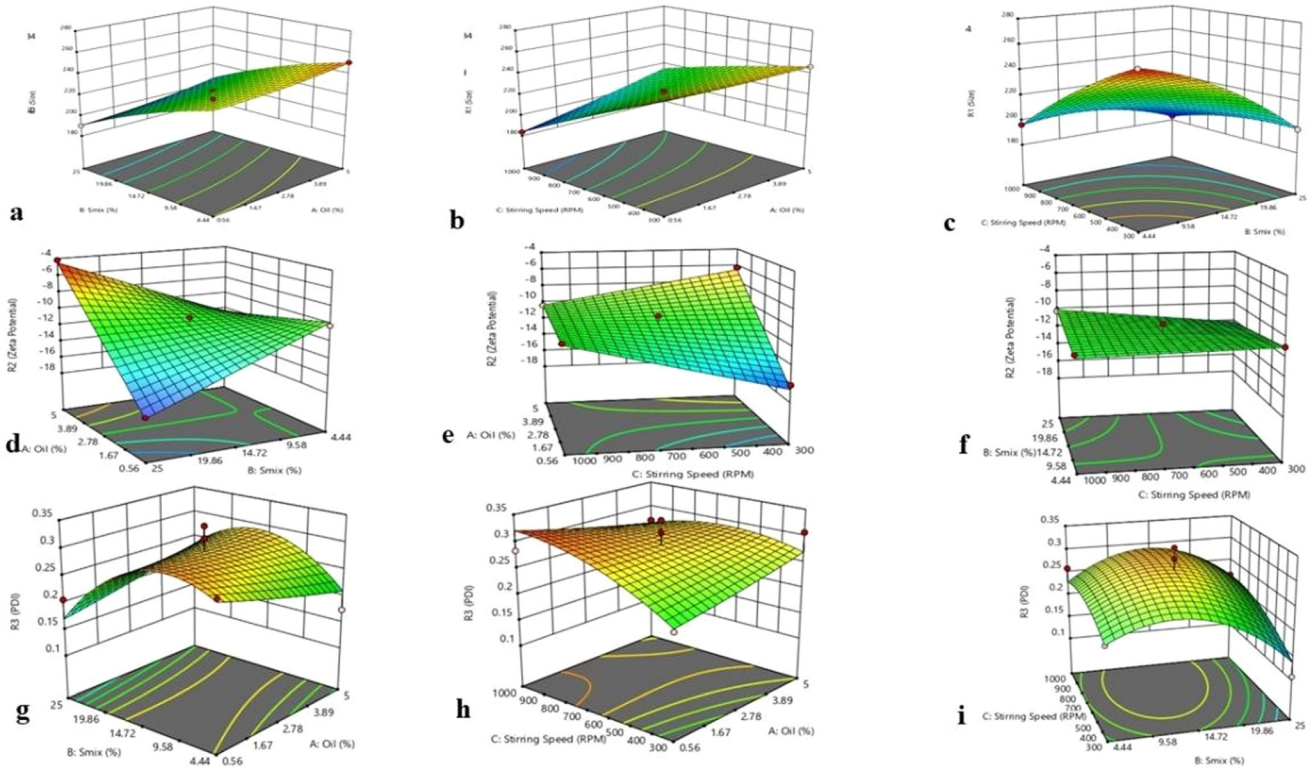

Fig. 3 The 3D response surface illustrating the interaction effect of independent variables, such as the oil concentration, S_{mix}, and stirring speed on the (a–c) particle size, (d–f) zeta potential, and (g–i) PDI.

Table 4 Stability testing parameters of different trials of NE formulation

S_{mix}	Batch no.	Turbidity	After 24 h turbidity.	Heating–cooling cycle	Centrifugation	Freeze thaw cycle
1 : 0	F1 (1 : 5)	N	N	x	—	—
1 : 0	F2 (1 : 7)	N	N	√	√	√
1 : 0	F3 (1 : 9)	N	N	√	√	√
1 : 0	F4 (1 : 8)	N	N	√	√	√
1 : 0	F5 (1 : 9)	N	N	√	√	√
1 : 1	F6 (1 : 6)	N	N	√	√	√
1 : 1	F7 (1 : 7)	N	N	√	√	√
1 : 1	F8 (1 : 8)	N	N	√	√	√
1 : 1	F9 (1 : 9)	N	N	√	√	√
1 : 1	F10 (1 : 9)	N	N	√	√	√
2 : 1	F11 (1 : 6)	N	N	x	—	—
2 : 1	F12 (1 : 7)	N	N	√	√	√
2 : 1	F 13 (1 : 8)	N	N	√	√	√
2 : 1	F 14 (1 : 9)	N	N	√	√	√
3 : 1	F15 (1 : 7)	N	N	√	√	√
3 : 1	F16 (1 : 8)	N	N	√	√	√
3 : 1	F17 (1 : 9)	N	N	√	√	√
4 : 1	F18 (1 : 8)	N	N	√	√	√
4 : 1	F19 (1 : 9)	N	N	√	√	√

√: pass; x: fail; N: No.

3.4 Characterization of the optimized NE

3.4.1 Particle size and polydispersity index (PDI). It was discovered that the nanometric range, or 186.2 nm, was obtained by the vesicles of the optimised NE produced by aqueous titration (Fig. 4). The PDI shows the homogeneity and size distribution of the dispersed particles in a formulation. A narrow size distribution is indicated by a PDI value between 0.1 and 0.3. In contrast, a PDI score greater than 0.4 suggests a wide size dispersion. The optimised NE's PDI was discovered to be 0.252 (Fig. 4), indicating a moderately polydisperse system as this PDI value is neither wide nor narrow.

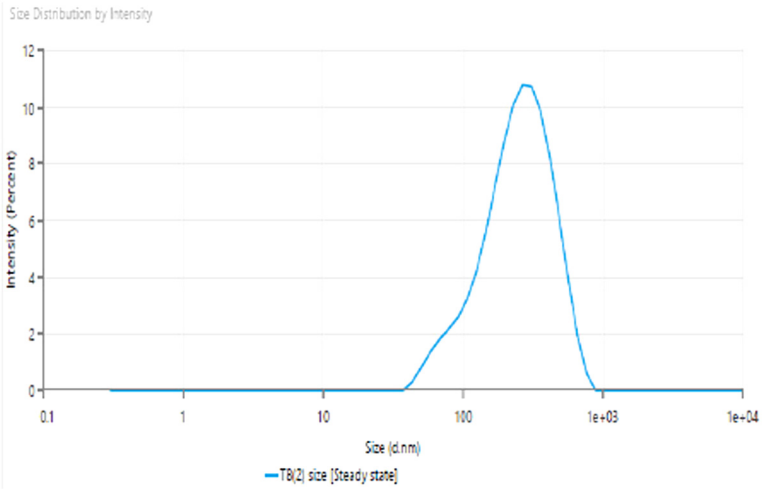

Statistics Table

Name	Mean	Standard Deviation	RSD	Minimum	Maximum
Z-Average (nm)	186.2	-	-	186.2	186.2
Polydispersity Index (PI)	0.252	-	-	0.252	0.252
Intercept	0.6973	-	-	0.6973	0.6973
Peak 1 Mean by Intensity ordered by area (nm)	137	-	-	137	137
Peak 1 Area by Intensity ordered by area (%)	100	-	-	100	100
Derived Mean Count Rate (kcps)	1184	-	-	1184	1184

Fig. 4 Particle size of vesicles of the optimised NE.

3.4.2 Zeta potential. Zeta potential analysis is a helpful method for determining whether a dispersed system is stable. It determines the degree of particle agglomeration brought on by electrostatic repulsion. Since non-ionic surfactants have more benefits than ionic or amphoteric surfactants in terms of stability, compatibility, reduced toxicity, and non-irritancy, they were used for the NE preparation. A negative zeta potential (Fig. 5) suggests high formulation stability, and the formulation's zeta potential was discovered to be −11.33 mV.

3.4.3 Morphology/transmission electron microscopy (TEM). After the optimized formulation was subjected to TEM analysis, a roughly spherical shape with a diameter of 180–200 nm was observed (Fig. 6). This size was in sync with what we observed in the Malvern Zetasizer. Little discrepancy in particle size may be the result of different sample preparation and principle analyses for the two procedures.

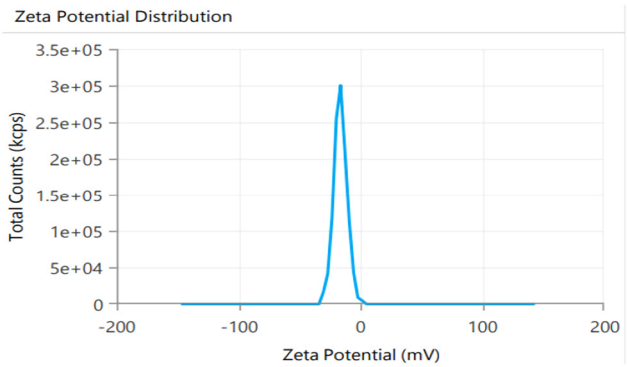

Fig. 5 Zeta potential of vesicles of the optimized NE.

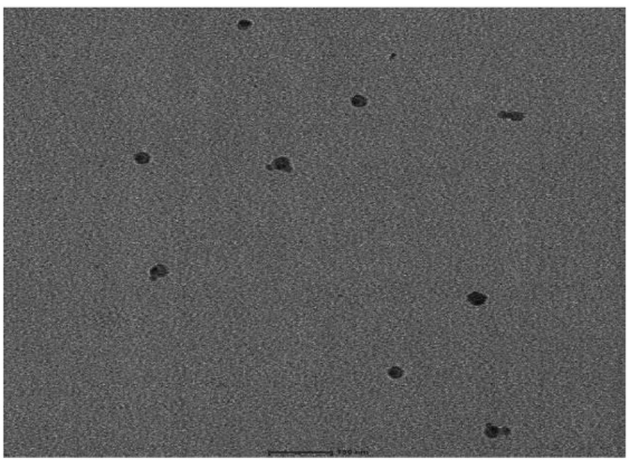

Fig. 6 TEM photomicrograph of NE depicting a size below 200 nm, along with the uniform shape of particles.

3.5 Preparation of oxaprozin loaded NEG

The best and most stable formulation was found to be a gel formulated with 1.5% w/v Carbopol in terms of appearance, texture, homogeneity, and spreadability. To the optimized gel formulation, 1% v/v glycerin was added as a humectant and 0.02% w/v methyl paraben as a preservative. It was also subjected to a variety of gel assessments and standards.

3.6 Evaluation of NEG

3.6.1 Drug content. One of the best qualities in a pharmaceutical formulation is a high drug content. The NEG's oxapro-

zin content was determined to be 92.1% ± 1.54%, corroborating the gelling agent selection.

3.6.2 Spreadability and extrudability. The oxaprozin-NEG that was optimised lacked a rough texture, and was uniformly smooth without any grit. The optimised gel's pH of 7.2 ± 0.32 suggests that it is safe and will not irritate the skin. Spreadability and extrudability play major roles in making it simple for application at the desired location and removal from the packet, respectively. Therefore, these are essential to maintain a high level of patient compliance. The optimised oxaprozin-NEG exhibits an extrudability of 1.8 ± 0.43 g cm^{-2} and a spreadability of 5.9 ± 0.155 g cm s^{-1} (Fig. 7).

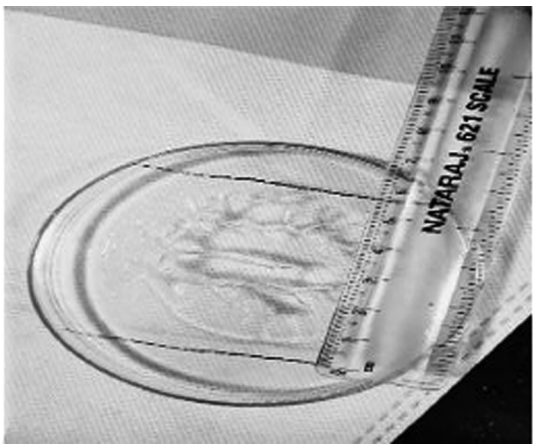

Fig. 7 Spreadability evaluation of the NEG in order to assess the amount of formulation expelled from the packaging.

3.6.3 Texture analysis of the placebo and formulation. Among the mechanical characteristics of the gel formulation are firmness, consistency, cohesiveness, and work of cohesion (Table 5). The applicability and patient compliance are directly impacted by these characteristics. The gel's firmness and consistency both show how sticky and strong the gel is. Better gel strength is indicated by a higher value. It was discovered that the optimised NEG (1.5% Carbopol) had the following values for firmness, consistency, cohesiveness, and work of cohesion: 200.29 g, 327.15 g s, −153.47 g, and −302.11 g s^{-1}, respectively. It was discovered that the optimised NEG possessed every property of the gel. For the formulation to be stable, packaged, and easy to use, the aforementioned textural qualities are essential. The texture curve revealed a uniformity and smoothness in the texture, which was observed to be free from grittiness and lumps (Fig. 8).

Table 5 Texture analysis data representing the values of firmness, consistency, cohesiveness and work of cohesion of NEG

Firmness (g)	Consistency (g s)	Cohesiveness (g)	Work of cohesion (g s^{-1})
200.29	327.13	−153.47	−302.11

3.6.4 Rheological behaviour studies. The prepared NEG exhibited a viscosity of 42.4 Pa s. The viscosity decreased as the shear rate increased from 0.1 s^{-1} to 100 s^{-1}, indicating a shear-thinning behavior characteristic of non-Newtonian pseudoplastic fluids. This reduction in viscosity at higher shear rates enables more efficient flow management, requiring less energy. Additionally, the NEG demonstrated enhanced thixotropic properties, suggesting potential industrial applications. As the NEG was sheared, the polymer network was disrupted, and microscopic gel layers were transferred to adjacent layers,

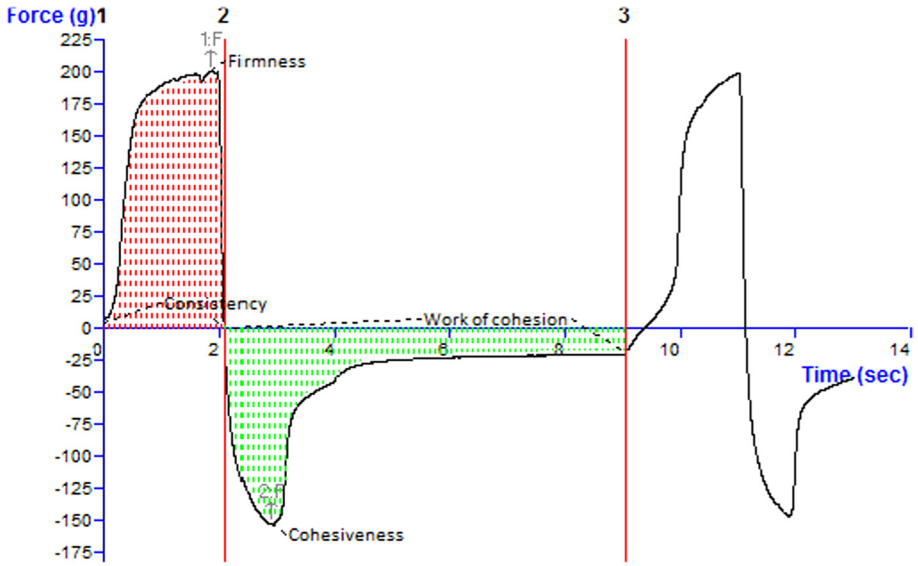

Fig. 8 Texture analysis data of the oxaprozin NE-gel. Cohesion work, cohesiveness, firmness, and consistency were calculated using the force-time plot. The cohesiveness of the gel is defined as the negative area under the force-time curve, whereas the maximum positive force indicates the gel's hardness or firmness.

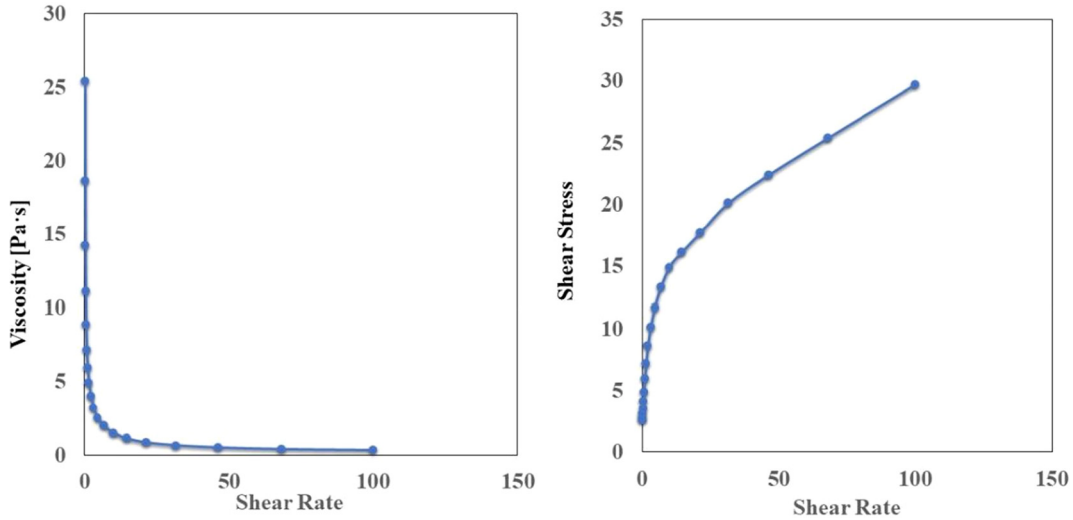

Fig. 9 Gel rheological measurements with the help of a rheometer at 25 °C with variations in the (1st) viscosity and (2nd) shear stress with respect to changes in the shear rate.

resulting in an increase in shear stress. Overall, these findings illustrate the shear-thinning behavior of the gel.[33]

3.6.5 Bioadhesive strength measurement. Bioadhesive strength of the oxaprozin-NEG was found to be 3.6 kg cm^{-2} (Fig. 9).

3.6.6 *In vitro* drug release study. *In vitro* release data provide preliminary evidence on the behavior of the formulation *in vivo*. The cumulative release profiles for the optimised formulation (oxaprozin-NEG) were created, computed, and graphically compared using a dialysis membrane, as indicated in Fig. 10. After 25 h, it was discovered that the percentage cumulative drug release for oxaprozin-NEG was 78.123% (Fig. 10). The optimised oxaprozin-NEG exhibited biphasic release behaviour, with a fast release pattern for the first five and a slow release after that. The first fast release may have been triggered by the drug's presence on the surface of the formulation, and the second slow release may have been caused by the drug becoming trapped in the gel matrix and impeding diffusion. Additionally, drug release in nanoemulsion is also affected by the interactions of the drug with the surfactants, and its distribution between the aqueous and oil phases. The sustained release pattern exhibited by the NEG has a greater advantage in the management of osteoarthritis. This would extend the retention time and improve the efficacy of the active constituents in the articular cavity. Furthermore, it would decrease the side effects by reducing the frequency of administration, hence improving the patient's compliance.[41]

3.6.7 *Ex vivo* skin permeation study. The skin of a recently excised rat was used for the *ex vivo* permeation tests (hair removal was done prior to sacrifice). The obtained oxaprozin-NE (9.476 μg cm^{-2} h^{-1}) permeation flux was compared to that of oxaprozin-NEG (6.564 μg cm^{-2} h^{-1}) (Fig. 11). Addition of oxaprozin-NE as a carrier to a gel system facilitates delivery and permeation, while enhancing the formulation stability.

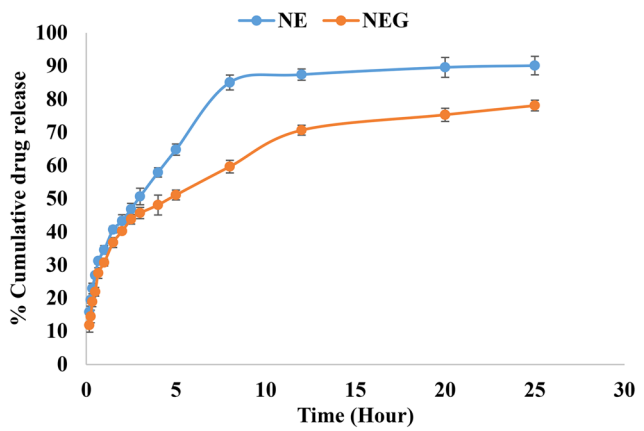

Fig. 10 *In vitro* release study profile of the NEG. Three duplicates of each study were conducted, and the results are displayed as mean ± SD.

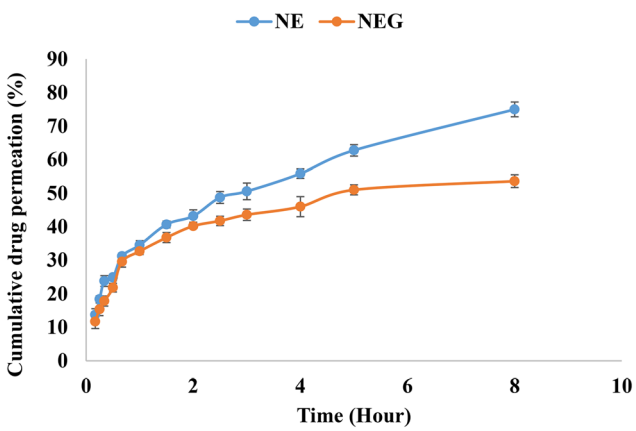

Fig. 11 *Ex vivo* drug permeation study profile of the NEG. Each study was performed in triplicates, and data are shown as mean ± SD.

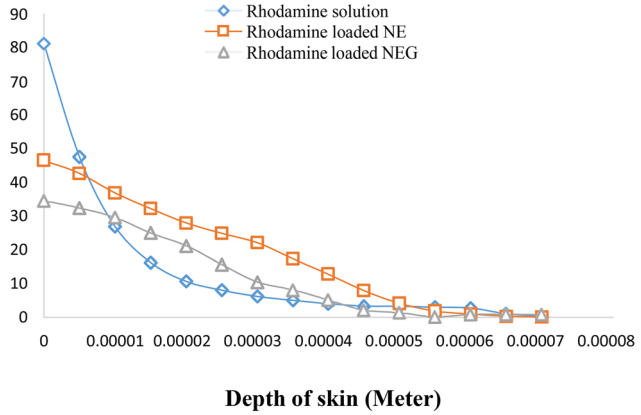

Fig. 12 CLSM comparison of rhodamine penetration between the rhodamine solution, NE and NEG.

Furthermore, a formulation's nanoscale size enhances its ability to penetrate the skin's natural layers, while also increasing drug retention.

3.6.3 CLSM study. The penetration of rhodamine dye through the skin at varying intensities from the formulations of Rhodamine B solution, Rhodamine B-laden NE, and Rhodamine B-laden NEG is depicted and compared in Fig. 12. Skin that has been laden with NE and NEG of rhodamine B fluoresces much brighter than skin that has been exposed to rhodamine solution. The high intensity of the rhodamine solution is caused by solubilization in a hydro-ethanolic mixture. Consequently, penetration may be enhanced by ethanol, which eventually became insignificant and lost intensity. Conversely, the burst release behaviour (observed in the *in vitro* release study) of the formulations in the case of rhodamine-loaded NE and NEG may have contributed to the initial increased fluorescence intensity in the skin for both cases. In the case of rhodamine-loaded NEG, the initial fluorescence intensity was comparatively less, but the depth of penetration was greater, demonstrating the success of the formulation. Notably, a robust fluorescence signal is observed between 10 and 50 μm, suggesting that the formulation has penetrated the stratum corneum. Given that the intact stratum corneum has a thickness ranging from 10 to 40 μm, it can thus be argued that the formulation passes through this layer and goes into the deeper layers of the skin. The result coincided with the study conducted by Zrien Naz *et al.*, who claimed that the nanoemulsion has a capability to alter the skin integrity and has a potential to permeate the skin by reducing inflammation in the joint.[42,43]

3.6.3 Skin irritation. The aim of this study was to make sure the formulation was suitable for topical application on the skin. Redness of the skin, which is caused by hyperemia of the superficial capillaries present on the surface of the skin, is called erythema. Edema is defined as swelling brought on by bodily tissue fluid. The erythema and oedema of the skin that were created at the application site were used to evaluate the study, and demonstrate how capable the formulation is of causing skin irritation. None of the animals showed any clinical sign related to skin irritation, and were assigned with a score of zero. Observations were made after particular time intervals. Even after 72 h (three days), neither the optimised NEG nor the NE irritated the application site, as observed after histological examinations of the dermis. Since the NE and NEG both have scores of zero, it can be concluded that they are not irritating and were topically safe (Fig. 13).

3.6.4 Stability study. The analysis of the NE and NEG's size, PDI, and drug content over the course of four weeks at

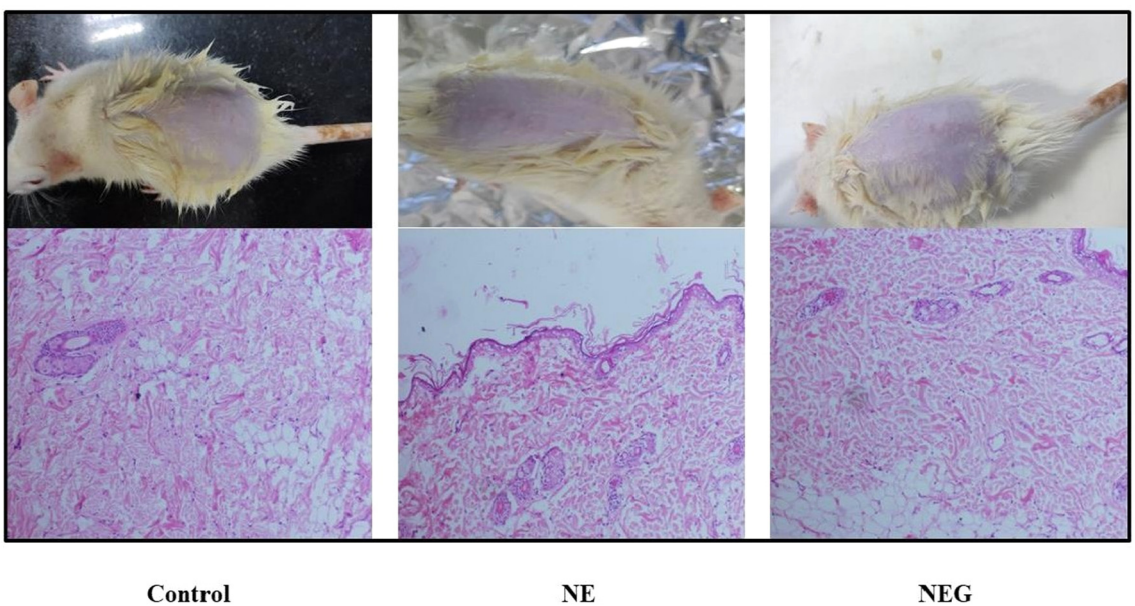

Fig. 13 Skin histological section of different animal groups showing no sign of inflammation.

Table 6 Stability study of the optimized NEG

	Nanoemulsion (NE)			Nanoemulgel (NEG)		
Time scale	Particle size	PDI	Drug content	Appearance	pH	Drug content
1st week	186.1	0.254	92.1	White viscous creamy	7.3 ± 0.05	92.1
2nd week	189.3	0.269	92.1	White viscous creamy	7.5 ± 0.07	92.0
3rd week	187.8	0.289	92.0	White viscous creamy	7.6 ± 0.09	92.0
4th week	190.7	0.296	92.0	White viscous creamy	7.8 ± 0.1	91.9

40 °C is compiled in Table 6. The relative stability was established for NE and NEG because neither a decrease in drug content nor an increase in size or PDI occurred. This indicates that the NE and NEG formulations were able to keep their size when kept in the right kind of storage with no drug leaking or leaching.

3. Conclusions

This research explored the formulation, characterization and evaluation of a nanoemulsion gel/nanoemulgel by aqueous titration method, employing the QbD optimization approach. Here, gaultheria oil is combined with oxaprozin to form a nanoemulgel for the management of osteoarthritis. The scientifically crafted nanoemulgel has a small vesicular size with good stability at 4 °C. It has a good drug content, *in vitro* release profile, bioadhesion and rheological properties with reduced skin irritancy. The formulation has a good permeation through the skin for effective delivery of active constituents, and can be established through a topical route. Hence, it is reasonable to assume that the optimised formulation has greater potential, and merits further study in preclinical and eventually clinical settings.

Author contributions

Conceptualization, Ahsan Ali, Mohd. Aamir Mirza, and Zeenat Iqbal; methodology, Talha, Sradhanjali Mohapatra and Uzma Farooq; software, Ayesha Siddiqui and Ramsha Ansari; formal analysis, Mohd. Aamir Mirza, and Zeenat Iqbal; investigation, Talha, and Ahsan Ali; resources Mohd. Aamir Mirza, and Zeenat Iqbal; writing, Talha, and Sradhanjali Mohapatra; writing – review and editing, Sradhanjali Mohapatra and Pooja Jain; project administration, Mohd. Aamir Mirza, and Zeenat Iqbal. All authors have read and agreed to the published version of the manuscript.

Institutional review board statement

The Institutional Animal Ethics Committee, Jamia Hamdard, New Delhi, India, approved protocol no. 1977 for Animal Studies (Registration No. 173/GO/Re/S/2000/CPCSEA, 21 December 2022).

Conflicts of interest

The authors declare no conflict of interest.

Acknowledgements

This research received no external funding. The authors are highly grateful to the Jamia Hamdard University, New Delhi, India for all its support.

References

1 R. Hamood, M. Tirosh, N. Fallach, G. Chodick, E. Eisenberg and O. Lubovsky, *J. Clin. Med.*, 2021, **10**, 1–11, DOI: 10.3390/jcm10184282.
2 S. Safiri, A. A. Kolahi, E. Smith, C. Hill, D. Bettampadi, M. A. Mansournia, D. Hoy, A. Ashrafi-Asgarabad, M. Sepidarkish, A. almasi-Hashiani, G. Collins, J. Kaufman, M. Qorbani, M. Moradi-Lakeh, A. D. Woolf, F. Guillemin, L. March and M. Cross, *Ann. Rheum. Dis.*, 2020, **10**, 1–10, DOI: 10.1136/annrheumdis-2019-216515.
3 K. Onishi, A. Utturkar, E. Chang, R. Panush, J. Hata and D. Perret-Karimi, *Crit. Rev. Phys. Rehabil. Med.*, 2012, **24**, 3–4, DOI: 10.1615/critrevphysrehabilmed.2013007630.
4 F. Zakir, S. Mohapatra, U. Farooq, M. A. Mirza and Z. Iqbal, *Drug Delivery Systems for Metabolic Disorders*, 2022, pp. 1–22.
5 A. Magni, P. Agostoni, C. Bonezzi, G. Massazza, P. Menè, V. Savarino and D. Fornasari, *Pain Ther.*, 2021, **10**, 783–808.
6 L. A. Salman, G. Ahmed, S. G. Dakin, B. Kendrick and A. Price, *Arthritis Res. Ther.*, 2023, **25**, 1–27.
7 R. L. Barkin, *Am. J. Ther.*, 2015, **22**, 388–407, DOI: 10.1097/MJT.0b013e3182459abd.
8 W. F. Kean, R. Kean and W. W. Buchanan, *Inflammopharmacology*, 2002, **10**, 241–284.
9 A. Weaver, B. Rubin, J. Caldwell, F. G. McMahon, D. Lee, W. Makarowski, H. Offenberg, M. Sack, D. Sikes, R. Trapp, S. Rush, M. Kuss, J. Ganju and T. S. Bocanegra, *Clin. Ther.*, 1995, **17**, 735–745, DOI: 10.1016/0149-2918(95)80050-6.
10 V. Gupta, S. Mohapatra, H. Mishra, U. Farooq, K. Kumar, M. J. Ansari, M. F. Aldawsari, A. S. Alalaiwe, M. A. Mirza and Z. Iqbal, *Gels*, 2022, **8**, 1–31.
11 M. R. Donthi, S. R. Munnangi, K. V. Krishna, R. N. Saha, G. Singhvi and S. K. Dubey, *Pharmaceutics*, 2023, **15**, 1, DOI: 10.3390/pharmaceutics15010164.

12 G. C. Aithal, R. Narayan and U. Y. Nayak, *Curr. Pharm. Des.*, 2020, **26**, 279–291, DOI: **10.2174/1381612826666191226100241**.
13 W. R. Liu, W. L. Qiao, Z. Z. Liu, X. H. Wang, R. Jiang, S. Y. Li, R. B. Shi and G. M. She, *Molecules*, 2013, **18**, 10, DOI: **10.3390/molecules181012071**.
14 M. Mukhopadhyay, P. Bantawa, T. K. Mondal and S. K. Nandi, *Ind. Crops Prod.*, 2016, **81**, 91–99, DOI: **10.1016/j.indcrop.2015.11.042**.
15 M. Marrelli, V. Amodeo, M. R. Perri, F. Conforti and G. Statti, *Plants*, 2020, **9**, 10, DOI: **10.3390/plants9101252**.
16 A. Veseli, S. Žakelj and A. Kristl, *Drug Dev. Ind. Pharm.*, 2019, **45**, 1717–1724, DOI: **10.1080/03639045.2019.1665062**.
17 M. Ganesh, B. Thangabalan, D. Thakur, K. Srinivasan, S. Ganguly and T. Sivakumar, *Asian – J. Chem.*, 2008, **7**, 5451–5454.
18 V. Bourganis, O. Kammona, A. Alexopoulos and C. Kiparissides, *Eur. J. Pharm. Biopharm.*, 2018, **128**, 337–362.
19 S. Baboota, A. Abdullah, G. Mustafa, J. K. Sahni and J. Ali, *J. Excipients Food Chem.*, 2013, **4**, 12–24.
20 K. Jain, R. Suresh Kumar, S. Sood and K. Gowthamarajan, *J. Pharm. Sci. Res.*, 2013, **5**, 1–18.
21 A. Gull, S. Ahmed, F. J. Ahmad, U. Nagaich and A. Chandra, *J. Drug Delivery Sci. Technol*, 2020, **57**, 1–11, DOI: **10.1016/j.jddst.2020.101641**.
22 A. G. Khidhir and A. S. Hamadi, *Adv. Chem. Eng. Sci.*, 2018, **08**, 1–24, DOI: **10.4236/aces.2018.83012**.
23 S. Beg, S. Swain, M. Rahman, M. S. Hasnain and S. S. Imam, in *Pharmaceutical Quality by Design: Principles and Applications*, 2019.
24 S. Beg, M. S. Hasnain, M. Rahman and S. Swain, in *Pharmaceutical Quality by Design: Principles and Applications*, 2019.
25 A. Azeem, M. Rizwan, F. J. Ahmad, Z. Iqbal, R. K. Khar, M. Aqil and S. Talegaonkar, *AAPS PharmSciTech*, 2009, **10**, 69–76, DOI: **10.1208/s12249-008-9178-x**.
26 M. S. Ali, M. S. Alam, N. Alam and M. R. Siddiqui, *Iran. J. Pharm. Res.*, 2014, **13**, 1125–1140.
27 S. Al-Jawadi and S. S. Thakur, *Int. J. Pharm.*, 2020, **585**, 1–55, DOI: **10.1016/j.ijpharm.2020.119559**.
28 F. Zakir, A. Ahmad, U. Farooq, M. A. Mirza, A. Tripathi, D. Singh, F. Shakeel, S. Mohapatra, F. J. Ahmad and K. Kohli, *Nanomedicine*, 2020, 1–21, DOI: **10.2217/nnm-2020-0079**.
29 Z. I. Anam Choudhary, P. Jain, S. Mohapatra, G. Mustafa, M. J. Ansari, M. F. Aldawsari, A. S. Alalaiwe and M. A. Mirza, *ACS Omega*, 2022, **7**, 15688–15694.
30 U. Farooq, M. A. Mirza, A. Alshetaili, S. Mohapatra, P. Jain and N. Hassan, *Nanoscale Adv.*, 2024, **6**, 648–668, DOI: **10.1039/D3NA00943B**.
31 S. Mohapatra, M. A. Mirza, S. Ahmad, U. Farooq, M. J. Ansari, K. Kohli and Z. Iqbal, *Pharmaceutics*, 2023, **15**, 1–25, DOI: **10.3390/pharmaceutics15020465**.
32 R. Khan, M. A. Mirza, M. Aqil, N. Hassan, F. Zakir, M. J. Ansari and Z. Iqbal, *Gels*, 2023, **8**, 1–24, DOI: **10.3390/gels8110733**.
33 S. Ansari, M. A. I. Rashid, P. R. Waghmare and D. S. Nobes, *SN Appl. Sci.*, 2020, **2**, 1–15, DOI: **10.1007/s42452-020-03561-w**.
34 M. Imran, M. K. Iqubal, K. Imtiyaz, S. Saleem, S. Mittal, M. M. A. Rizvi, J. Ali and S. Baboota, *Int. J. Pharm.*, 2020, 1–17, DOI: **10.1016/j.ijpharm.2020.119705**.
35 S. S. Sultana, P. Parveen, M. Sri Rekha, K. Deepthi, C. A. Sowjanya, D. Seetha and S. S. Sultana, *Indo Am. J. Pharm. Res*, 2017, 1–32, DOI: **10.1016/j.xphs.2017.03.042**.
36 J. Luan, F. Zheng, X. Yang, A. Yu and G. Zhai, *Colloids Surf., A*, 2014, 1–27, DOI: **10.1016/j.colsurfa.2014.11.015**.
37 C. S. Weil and R. A. Scala, *Toxicol. Appl. Pharmacol.*, 1970, **19**, 276–360, DOI: **10.1016/0041-008X(71)90112-8**.
38 Jyotshna, A. Chand Gupta, D. U. Bawankule, A. K. Verma and K. Shanker, *J. Drug Delivery Sci. Technol.*, 2020, **57**, 1–9, DOI: **10.1016/j.jddst.2020.101734**.
39 C. Thapa, A. Ahad, M. Aqil, S. S. Imam and Y. Sultana, *J. Drug Delivery Sci. Technol.*, 2018, 4–35, DOI: **10.1016/j.jddst.2018.02.003**.
40 D. Patel, M. Patel, T. Soni and B. Suhagia, *J. Drug Delivery Sci. Technol*, 2021, **61**, 1–15, DOI: **10.1016/j.jddst.2021.102329**.
41 P. Suresh, M. M. Salem-Bekhit, H. P. Veedu, S. Alshehri, S. C. Nair, S. I. Bukhari, V. Viswanad, E. I. Taha, R. K. Sahu, M. M. Ghoneim and I. Elbagory, *Nanomaterials*, 2022, **12**, 1–16, DOI: **10.3390/nano12081299**.
42 Z. Naz and F. J. Ahmad, *Int. J. Nanomed.*, 2015, 1–15, DOI: **10.2147/IJN.S82788**.
43 M. S. Khan, S. Mohapatra, V. Gupta, A. Ali, P. P. Naseef, M. S. Kurunian, A. A. F. Alshadidi, M. S. Alam, M. A. Mirza and Z. Iqbal, *Membranes*, 2023, **13**, 1–30, DOI: **10.3390/membranes13030343**.